ACCEPTED FOR PUBLICATION BY *The Astrophysical Journal*
Preprint typeset using LaTeX style emulateapj v. 14/09/00

A MILLISECOND PULSAR OPTICAL COUNTERPART WITH LARGE-AMPLITUDE VARIABILITY IN THE GLOBULAR CLUSTER 47 TUCANAE [1]

PETER D. EDMONDS[2], RONALD L. GILLILAND[3], FERNANDO CAMILO[4], CRAIG O. HEINKE[2] AND JONATHAN E. GRINDLAY[2]
Accepted for publication by The Astrophysical Journal

ABSTRACT

Using extensive *HST* imaging, combined with *Chandra* X-ray and Parkes radio data, we have detected the optical binary companion to a second millisecond pulsar (MSP) in the globular cluster 47 Tucanae. This faint ($V = 22.3$) blue ($V - I = 0.7$) star shows a large amplitude (60–70%) sinusoidal variation in both V and I. The period (3.19066 hr) and phase of the variation match those of the MSP 47 Tuc W (which does not have an accurate radio timing position) to within 0.5 seconds and 1.2 minutes respectively, well within the 1 σ errors. The phase dependence of the intensity and color implies that heating of a tidally locked companion causes the observed variations. The eclipsing nature of this MSP in the radio, combined with the relatively large companion mass (> 0.13 $M_\odot$) and the companion's position in the color-magnitude diagram, suggest that the companion is a main sequence star, a rare circumstance for an MSP companion. This system is likely to have had a complex evolution and represents an interesting case study in MSP irradiation of a close companion. We present evidence for another optical variable with similar properties to the companion of 47 Tuc W. This variable may also be an MSP companion, although no radio counterpart has yet been detected.

Subject headings: binaries: general — globular clusters: individual (47 Tucanae) — techniques: photometric — pulsars: individual (PSR J0024–7204W) — pulsars: general

1. INTRODUCTION

More than 50 millisecond pulsars (MSPs), half of all known, have been found in radio surveys of globular clusters, where the high stellar densities and interaction rates cause large numbers of neutron stars (NSs) to be spun up to millisecond periods (via binary production and subsequent accretion onto the compact object). Studies of these objects therefore offer insight into the formation and evolution of NS binaries (see, e.g., Rasio, Pfahl, & Rappaport 2000) and the frequency of stellar interactions in the dense cores of clusters, sampling different evolutionary channels compared to the disk population.

Recent improvements in the sensitivity of the Parkes radio telescope have resulted in a dramatic increase in the number of cluster MSPs detected. In particular, the 11 known MSPs in the cluster 47 Tuc (Manchester et al. 1991; Robinson et al. 1995) have recently been increased to 20 (Camilo et al. 2000, hereafter CLF00), with 16 of these currently having accurate (milli-arcsecond) timing positions (Freire et al. 2001a; Freire 2001). These enable studies of the cluster's gravitational potential well (Freire et al. 2001a) and of the intra-cluster medium (Freire et al. 2001b).

Another significant observational advance has been the ability of *Chandra* to detect cluster MSPs in large numbers (Grindlay et al. 2001a, 2002; D'Amico et al. 2002). Accurate ($0''.1$–$0''.2$) X-ray positions for the MSPs combined with the detection of large numbers of cataclysmic variables (CVs) and active binaries with both *Chandra* and *HST* (Grindlay et al. 2001a and Edmonds et al. 2002a, in preparation) has allowed the radio, X-ray and optical data to be placed on a common astrometric frame, good to $\lesssim 0''.1$.

These advances, and the superb spatial resolution of *Chandra* and *HST*, have allowed the recent detection of two optical counterparts to cluster MSPs, PSR J0024–7203U, hereafter 47 Tuc U, in 47 Tuc (Edmonds et al. 2001a, hereafter EGH01), and PSR J1740–5340, hereafter NGC 6397 A, in NGC 6397 (Ferraro et al. 2001). The MSP 47 Tuc U has a $\sim$0.15 $M_\odot$ He white dwarf (WD) companion, a 10.3 hr binary period and small amplitude (0.004 mag in V) orbital variations caused by heating of one side of the companion (EGH01). The $\sim$0.45 $M_\odot$ companion in NGC 6397 A is either a subgiant or a heated main sequence (MS) star (Ferraro et al. 2001). The 32.5 hr, 0.1 mag orbital variations are caused by tidal distortion of the secondary by the NS, and are roughly sinusoidal with a (32.5/2) hr period. Another notable feature of NGC 6397 A is that the spectrum of the X-ray counterpart is relatively hard, and is suggestive of non-thermal emission. By contrast, 8 out of 9 of the 47 Tuc MSPs which are bright enough to have useful spectral information are soft (Grindlay et al. 2002).

Currently, NGC 6397 A appears to be unique among known MSPs in having a likely non-degenerate companion. The MSPs in 47 Tuc, for example, are either single, have likely He WD companions (e.g. 47 Tuc U), or have secondaries with masses of $\sim$0.02–0.03 $M_\odot$ (CLF00) which cannot be normal MS stars. As argued by Burderi et al. (2002) and Ferraro et al. (2001), the subgiant companion to NGC 6397 A may have been the star that recently spun up the MSP, consistent with the relatively small (characteristic) age for the system (D'Amico et al. 2001). The position of the star in the color-magnitude diagram (CMD) is roughly consistent with that of a mass-losing subgiant like that in the CV AKO 9 in 47 Tuc (Albrow et al. 2001). The equally interesting possibility presented by Ferraro et al. (2001) is that an MS star has been captured in an exchange interaction with an NS already spun-up to millisecond periods. Further work is

[1] Based on observations with the NASA/ESA *Hubble Space Telescope* obtained at STScI, which is operated by AURA, Inc. under NASA contract NAS 5-26555.

[2] Harvard-Smithsonian Center for Astrophysics, 60 Garden St, Cambridge, MA 02138; pedmonds@cfa.harvard.edu; cheinke@cfa.harvard.edu; josh@cfa.harvard.edu

[3] Space Telescope Science Institute, 3700 San Martin Drive, Baltimore, MD 21218; gillil@stsci.edu

[4] Columbia Astrophysics Laboratory, Columbia University, 550 West 120th Street, New York, NY 10027; fernando@astro.columbia.edu

needed to test whether the position of the star in the CMD is consistent with estimates of heating of the companion by the MSP (Ferraro et al. 2001). The relatively large amplitude of the ellipsoidal variations in NGC 6397 A suggests a high inclination orbit (Ferraro et al. 2001; Orosz & van Kerkwijk 2002), consistent with the detection of eclipses in the radio (D'Amico et al. 2001).

Five out of eight eclipsing MSPs known have very low companion masses of $\sim$0.02–0.03 $M_{\odot}$, and short orbital periods (these include the 47 Tuc MSPs J, O, and R). The three exceptions are NGC 6397 A; PSR B1744–24A in the cluster Terzan 5, with an orbital period of $\sim$1.8 hr, companion mass $\sim$0.10 $M_{\odot}$, and displaying irregular eclipses (Lyne et al. 1990); and 47 Tuc W, an eclipsing MSP in 47 Tuc with a $\sim$3.2 hr period but with a companion mass of $\sim$0.15 $M_{\odot}$ (CLF00; see § 2.1).

We present here extensive *HST* evidence for an optical counterpart to 47 Tuc W based on the detection of a faint, large amplitude, optical variable with an orbital period and phase which perfectly match those of 47 Tuc W within the uncertainties. The X-ray counterpart detected with *Chandra* has properties which are similar to those of NGC 6397 A. This detection represents the best evidence yet obtained for an MSP with an MS companion, given uncertainties about the evolutionary status of NGC 6397 A. Following a brief summary of the radio data available on 47 Tuc W, we present the astrometry, absolute photometry and time series photometry for the 47 Tuc W optical companion in § 2, where we also present evidence for a 2nd possible MSP companion with similar optical and X-ray properties. In § 3 we discuss the implications of these results.

2. OBSERVATIONS, DATA ANALYSIS, AND RESULTS

2.1. *Radio Data*

The 2.35 ms pulsar 47 Tuc W was discovered on 1999 February 5 (MJD 51214) during a $\sim$4 hr observation with the Parkes radio telescope (CLF00). It has never been detected again (which happens for a few very weak pulsars that are detected seldom and only due to the focusing effects of interstellar scintillation), and hence has no position determined from radio timing measurements. However, that one observation was sufficient to determine that it is part of a binary system with a period of $\sim$3.2 hr, owing to the varying apparent spin period caused by Doppler shift. The times-of-arrival (TOAs) determined from the discovery data can be used to obtain precise orbital parameters.

We have used 40 good TOAs together with the TEMPO[5] timing software to measure an accurate barycentric pulsar spin period, projected semi-major axis of 0.2434(1) light-sec, binary period P_b = 0.13295(4) days, and time of pulsar ascending node T_0 = 51214.284829(3) MJD, where all uncertainties given are conservative (10$\times$ TEMPO), accounting for covariances in fitted parameters. The orbit is circular, with eccentricity < 0.001. With orbital phase (ϕ_b) zero defined at T_0, the pulsar is clearly eclipsed during $0.1 < \phi_b < 0.4$ (hereafter we redefine the fiducial point of orbital phase such that $\phi_b = 0$ at $T_{max} \equiv T_0 + [3/4]P_b$, retaining the binary phase convention used by EGH01). With the measured orbital parameters, and assuming an NS mass of 1.4 $M_{\odot}$, the pulsar mass function implies a companion mass > 0.13 $M_{\odot}$, with a mass of $\sim$0.15 $M_{\odot}$ for an orbital inclination of 60°.

[5] See http://pulsar.princeton.edu/tempo.

2.2. *Summary of Optical Data*

The optical data used in this paper consists of four different *HST* programs, GO-8267, GO-7503, GO-8219, and SM3/ACS-9028, summarized in Table 1. The program GO-8267 (PI R. Gilliland) involved an extensive set of 160 s Wide Field Planetary Camera 2 (WFPC2) exposures in F555W (636 images) and F814W (653) obtained over 8.3 days in 1999 July. A limited number (28) of F336W exposures were also obtained (not shown in Table 1). The use of these data to search for transiting planets and to study binaries are described in Gilliland et al. (2000) and Albrow et al. (2001) respectively. The program GO-7503 (PI G. Meylan) involved a short set of dithered F555W exposures with WFPC2 taken over three orbits about 110 days after GO-8267. The GO-8219 (PI C. Knigge) data consisted of six blocks of eight 30 s exposures each using the Space Telescope Imaging Spectrograph (STIS) in CCD mode with the so-called CLEAR filter (two exposures of one visit were lost resulting in 46 total exposures). The high throughput of STIS/CCD resulted in comparable count levels for faint stars in 30 s compared to the 160 s F555W and F814W WFPC2 exposures. The first visit of GO-8219 was about 65 days after GO-8267, while the remaining five visits were over a 10 day period some 401 days after GO-8267. Finally, SM3/ACS-9028 consisted of 20 cosmic ray split observations of 120 s with the F475W filter using the High Resolution Camera (HRC) of the newly installed Advanced Camera for Surveys (ACS) on *HST*. These data were acquired with 20 large-scale dithers over 4 orbits of *HST* as calibration of the camera's geometric distortion, and were obtained in 2002 April about 1002 days after GO-8267.

2.3. *W29 and Chandra–HST Astrometry*

The astrometry between *Chandra* and *HST*, based on the GO-8267 data, has already been described in EGH01 and Edmonds et al. (2002b). A partial set of optical identifications was described by Grindlay et al. (2001a) and the full set is described in Edmonds et al. (2002a, in preparation). This paper focuses on the optical identification for the X-ray source W29 from Grindlay et al. (2001a). We first establish the similarity of this source to some known X-ray counterparts of MSPs, and then present the *Chandra–HST* astrometry.

The low luminosity and relatively hard X-ray spectrum of W29 are similar to those of U12 (the X-ray counterpart of NGC 6397 A; Grindlay et al. 2001b) and 47 Tuc J, both eclipsing MSP binaries (see Grindlay et al. 2002). The X-ray spectrum of W29 can be best fit with a power law (photon index = 1.8$\pm$0.6 when fixing N_H to the nominal cluster value; χ^2_ν = 1.55) and the luminosity in the 0.5–2.5 keV band is 7.8×10^{30}erg s^{-1}. By comparison, for U12 a power law fit gives a photon index of 1.6$\pm$0.3 (when fixing N_H to the cluster value) and a luminosity of 4×10^{30}erg s^{-1}. Because both W29 and U12 are relatively faint sources (41 and 66 counts respectively), these X-ray sources are also consistent with $\sim$6 keV thermal bremsstrahlung spectra (χ^2_ν = 1.94 for W29). The X-ray counterpart of 47 Tuc J, W63, has only 10 counts ($L_x = 1.8 \times 10^{30}$erg s^{-1}) and is too faint for useful spectral fitting, but has hardness ratios consistent with a power law of photon index between 1 and 1.5 (Grindlay et al. 2002).

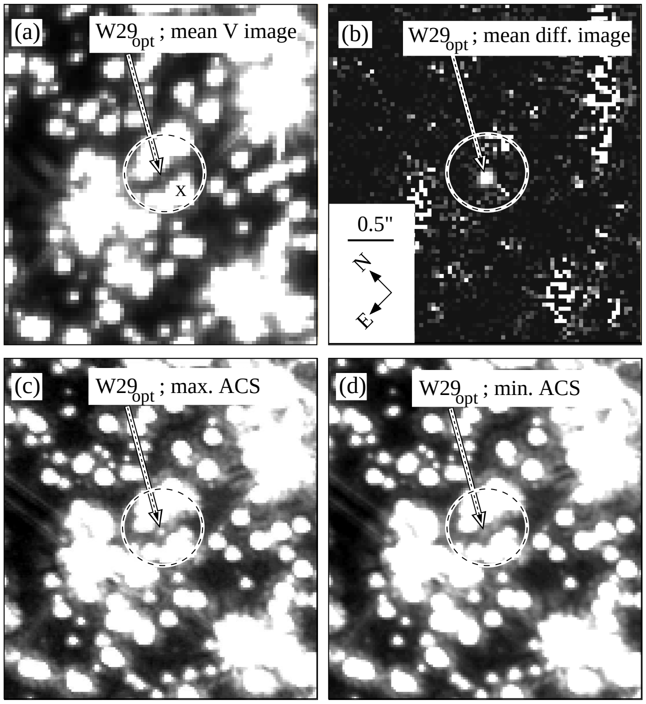

FIG. 1.— *HST* finding charts for W29$_{opt}$, using the GO-8267 (V) and SM3/ACS-9028 (F475W) data. The mean direct image from GO-8267 (WFPC2) is shown in Fig. 1a and the mean difference image is shown in Fig. 1b (see text for definitions). The ACS/HRC image for W29$_{opt}$ near maximum (ϕ_b = 0.0±0.16) is shown in Fig. 1c and the corresponding image near minimum (ϕ_b = 0.5±0.16) in Fig. 1d. The 5 σ (0.″42) error circle for W29 is shown, as is the scale and orientation of the *HST* images. The variable, optical counterpart for W29 (denoted W29$_{opt}$) is clearly visible near the center of the X-ray error circle in the mean difference and maximum ACS images (labeled with an arrow), but is barely visible in the mean direct and minimum ACS images. The initial identification for the ∼3.2 hr variable (PC1-V46) is labeled with 'X'.

A plausible optical counterpart for W29 was identified as a nearby 3.187 hr period variable. The variations in this very crowded region were initially believed to arise from a relatively bright star (U = 18.37, V = 17.79 and I = 17.13), identified as a non-eclipsing contact binary with an orbital period of 6.374 hr, and an amplitude of ∼0.002 mag (PC1-V46 from Albrow et al. 2001). This star is located 0.″25 (3.0 σ) from W29, where the astrometric uncertainty standard deviation σ is a combination of positional errors for W29 and small systematic errors in transforming between the *Chandra* and *HST* coordinate frames. However, a careful examination of the directly observed images ('direct images'; a term used to describe both individual exposures and mean images) and difference images[6] showed that the bright star identified as PC1-V46 was not the true variable. Instead, there is a faint, nearby star (only 0.″19 away) with a much larger intrinsic variability amplitude. This star was not included in our original star lists because it is faint and very crowded (it lies only 3.″8, or 16% of the core radius, r_c, away from the cluster center), but it fell within, and hence contaminated, the aperture used for PC1-V46. The new variable will be designated W29$_{opt}$ since it is only 0.″07 (0.8 σ) away from W29. The likelihood that this positional match is a coincidence is very low. On the PC chip there are 39 variables from Albrow et al. (2001) with V fainter than the MS turnoff, so the probability of a chance match between W29 and an optical variable is only $\sim 5\times10^{-4}$. The position of W29$_{opt}$ in the astrometric coordinate system of the MSPs (based on the JPL DE200 planetary ephemeris; Freire et al. 2001a) is given in Table 2.

The time series for W29$_{opt}$ is approximately sinusoidal with an amplitude of 70% in the V-band and 60% in the I-band. More details on the time series will be given in § 2.5. Here, we use the phase information for W29$_{opt}$ to construct mean direct and difference images for this variable. Figure 1a shows the average of direct images within ±0.07 in orbital phase of ϕ_b = 0.0 (maximum light) and within ±0.07 of ϕ_b = 0.5 (minimum light) in the W29$_{opt}$ time series, where we use the binary phase convention given in § 2.1. This provides an average intensity direct image for the variable without over-sampling. The variable W29$_{opt}$ is barely visible about 1 pixel below the center of the 5 σ X-ray error circle for W29. Clearly, W29$_{opt}$ is located in a crowded region of 47 Tuc even at *HST* resolution. Although there are no other identifiable stars within a 0.″1 radius of W29$_{opt}$, within a radius of 0.″2 there are three stars with a total intensity in F555W over 200 times that of W29$_{opt}$, and within a 0.″5 radius a total of 13 stars have a total intensity nearly 800 times that of W29$_{opt}$. Since W29$_{opt}$ has a color comparable to cluster turnoff stars (see § 2.4), while most stars are redder than this, the relative brightness of nearby stars is somewhat higher yet in F814W or the STIS CLEAR filter bandpass.

Figure 1b shows the sum of all difference images within ±0.07 of ϕ_b = 0.0, minus the sum of all difference images within ±0.07 of ϕ_b = 0.5, giving the mean difference image. Non-variables disappear except for noise. Note the clear detection of W29$_{opt}$ near the center of the X-ray error circle and coincident with a faint, relatively blue star just visible in the mean direct image. The large variability of W29$_{opt}$ is shown by comparing the two ACS/HRC images shown near maximum (ϕ_b = 0.0±0.16) and minimum (ϕ_b = 0.5±0.16). The absolute photometry for this star will now be described.

2.4. *Photometry*

Because of the extreme crowding described in § 2.3, the absolute photometry for W29$_{opt}$ requires special attention and we have used two different methods to estimate the U, V and I magnitudes for this star:

(*i*) We constructed direct images for W29$_{opt}$ at maximum (ϕ_b = 0.0±0.16) and minimum (ϕ_b = 0.5±0.16) in V and I, and subtracted the minimum image away from both the maximum and the mean images. In each of these two residual images, W29$_{opt}$ was much more clearly visible than in any of the direct images, and crowding was no longer a limiting factor in the photometry. After carrying out point spread function (PSF) fitting to the W29$_{opt}$ neighbors in the mean image, we applied this PSF-fitting to W29$_{opt}$ in the residual images, and used the measured light curves to derive V and I magnitudes for W29$_{opt}$ at ϕ_b = 0.0, ϕ_b = 0.5, and mean values averaged over the complete GO-8267 dataset. For U a mean value only was derived using this technique, because of the much lower signal-to-noise ratio. Mean values of $U = 23.8\pm0.5$, $V = 22.3\pm0.2$ and $I = 21.6\pm0.3$ were derived (see Table 2), where the errors are a combination of uncertainties from the PSF-fitting and estimated absolute errors in the conversion from *HST* to Johnson magnitudes.

(*ii*) The second technique involved use of the deep, oversampled images, the accurately known position for W29$_{opt}$, and

[6] difference images are generated by subtracting from each individual direct image the mean over-sampled image evaluated at the appropriate dither position; see Albrow et al. 2001

local sky determinations, to estimate the peak intensity levels for $W29_{opt}$ in the three different filters. We then scaled these values to Johnson *UVI* magnitudes using nearby stars and the PSF-fitting results of Gilliland et al. (2000). Mean values of $U = 23.7 \pm 0.7$, $V = 22.4 \pm 0.2$ and $I = 21.7 \pm 0.3$ were derived, in good agreement with the values from (*i*).

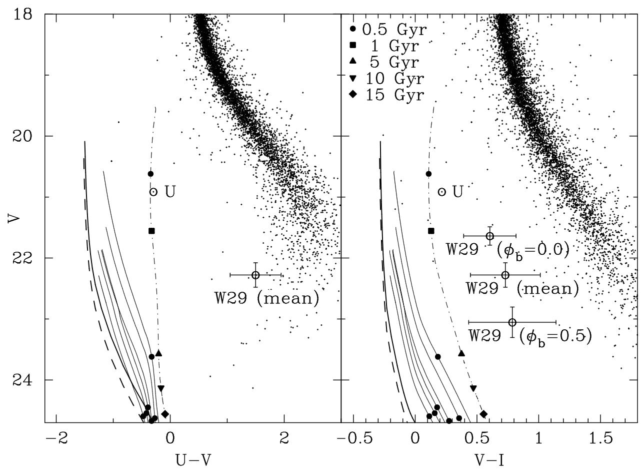

FIG. 2.— *HST* CMDs for GO-8267 based on PSF-fitting. The variable $W29_{opt}$ and the counterpart to the MSP 47 Tuc U ('U'; EGH01) are labeled. The thicker lines show Bergeron, Wesemael, & Beauchamp (1995) models for 0.5 $M_\odot$ (dashed line) and 0.6 $M_\odot$ (solid line) CO WDs. The thinner lines are Serenelli et al. (2001) models, for He WD masses of 0.406, 0.360, 0.327, 0.292, 0.242, 0.196 $M_\odot$, with mass decreasing towards the red, and 0.169 $M_\odot$ (dot-dashed line). Cooling ages are as shown. These models have been plotted assuming that $(m-M)_0 = 13.27$, the mean of the 9 distance modulus values reported in Zoccali et al. (2001), $E(B-V) = 0.055$ (Zoccali et al. 2001), $A_U/A_V = 1.51$ and $A_I/A_V = 0.60$ (Holtzman et al. 1995). Using $(m-M)_0 = 13.27$ the distance to 47 Tuc is 4.5 kpc.

Figure 2 shows the V vs $U-V$ and V vs $V-I$ CMDs for the PC chip, with $W29_{opt}$ labeled. The known counterpart to MSP 47 Tuc U (EGH01) is also shown. All of the points in the CMDs, including $W29_{opt}$ (where the photometry from [*i*] was used), had magnitudes which were self-consistently determined by PSF fitting. The various plotted lines are the CO WD cooling tracks of Bergeron et al. (1995) and the He WD cooling tracks of Serenelli et al. (2001). Note that the colors of $W29_{opt}$ appear to be inconsistent with those of any He WD cooling track, unlike the case for 47 Tuc U.

2.5. *Time Series*

2.5.1. *GO-8267 data*

The original time series analysis, upon which the initial possible match of $W29_{opt}$ with the MSP 47 Tuc W was made, used only the GO-8267 data. Here, we applied the standard difference image technique (see Gilliland et al. 2000 and Albrow et al. 2001) using a circular aperture, for this crowded target star, with an area of only 5 pixels (1 pixel = $0''.045 \times 0''.045$) to minimize contamination from neighboring companions. The top panel of Figure 3 shows the full time series for $W29_{opt}$, and the middle and bottom panels show the GO-8267 data with a sinusoidal fit superimposed (the *I*-band light curve has been scaled by a factor of 1.17 so that V and I have the same amplitude). The times displayed in the x-axis were derived by extracting the Modified Julian Date (MJD) of the observations, given in Universal Time, from the *HST* FITS headers, and converting to Heliocentric Julian Date (HJD) using the IRAF task `rvcorrect`[7]. The y-axis units are fractional intensity, defined as (intensity$-$<intensity>)/<intensity> (where <intensity> is the mean intensity). This system is used because it is linear (unlike the magnitude system) and gives light curves for $W29_{opt}$ which correctly appear sinusoidal for an intrinsic sinusoidal modulation.

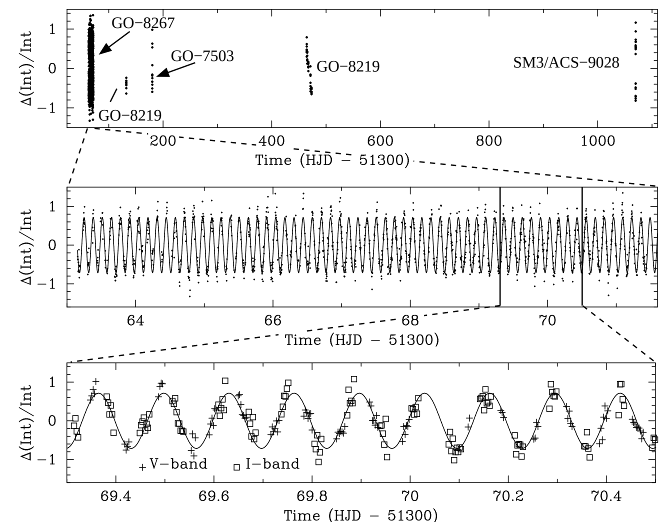

FIG. 3.— *HST* time series for $W29_{opt}$. The top panel shows the full set of time series analyzed here (the different datasets are labeled), extending from 1999 July to 2002 April. The times shown are extracted from the *HST* FITS headers. The middle panel shows the GO-8267 data and the bottom panel shows a close-up of a typical sample of the GO-8267 data (a sinusoidal fit to the data is shown in each case). The *I*-band data has been scaled so that its amplitude equals that of the *V*-band data. In the bottom panel different symbols have been used for the two filters.

We then performed a simultaneous least-squares fit of the GO-8267 V and I data to a sinusoid, allowing the amplitude, period and time of optical maximum ($T_{max} \equiv T[\phi_b = 0.0]$) to vary. The following values were obtained: amplitude = 0.714(9), $P_b = 0.132919(16)$ d, and $T_{max} = 51366.87064(28)$ MJD (all T_{max} values are given in barycentric MJD to within a small error of 1–2 s). Because of the difficult photometry for $W29_{opt}$ there is an additional $\sim$20% error for the amplitude resulting from assumed normalization using the mean absolute magnitude.

We now compare these results with the measured radio parameters of 47 Tuc W. The orbital period of 47 Tuc W (see § 2.1 and Table 2) differs from the period of $W29_{opt}$ by only 0.00003 d (2.7 s, a 0.02% relative difference), a difference of 0.8 σ when using the larger (radio) error. The radio value for T_{max} (when the heated hemisphere of $W29_{opt}$ is facing towards the Sun and is expected to be brightest, in a model where $W29_{opt}$ is heated by the pulsar wind) is 51214.38454(3) barycentric MJD (Table 2). By projecting the optically-derived T_{max} backwards in time by 1147 orbits, we derive $T_{max} = 51214.412(18)$ MJD. This differs from the radio-inferred T_{max} by (0.028 $\pm$ 0.018) d, a 40 minute difference (0.2 in phase). These results suggest that $W29_{opt}$ may be the companion to 47 Tuc W, although the phase errors are still relatively large. These errors are significantly reduced in § 2.5.2 with the use of archival data.

The phase plots and Lomb-Scargle (Scargle 1982) power spectra for $W29_{opt}$ in the V and I bands are shown in Figure 4.

[7] HJD differs from barycentric MJD by a variable heliocenter–barycenter light travel time of $\sim$1–2 s, in addition to a trivial 0.5 d offset due to a different zero-point definition of the two time scales.

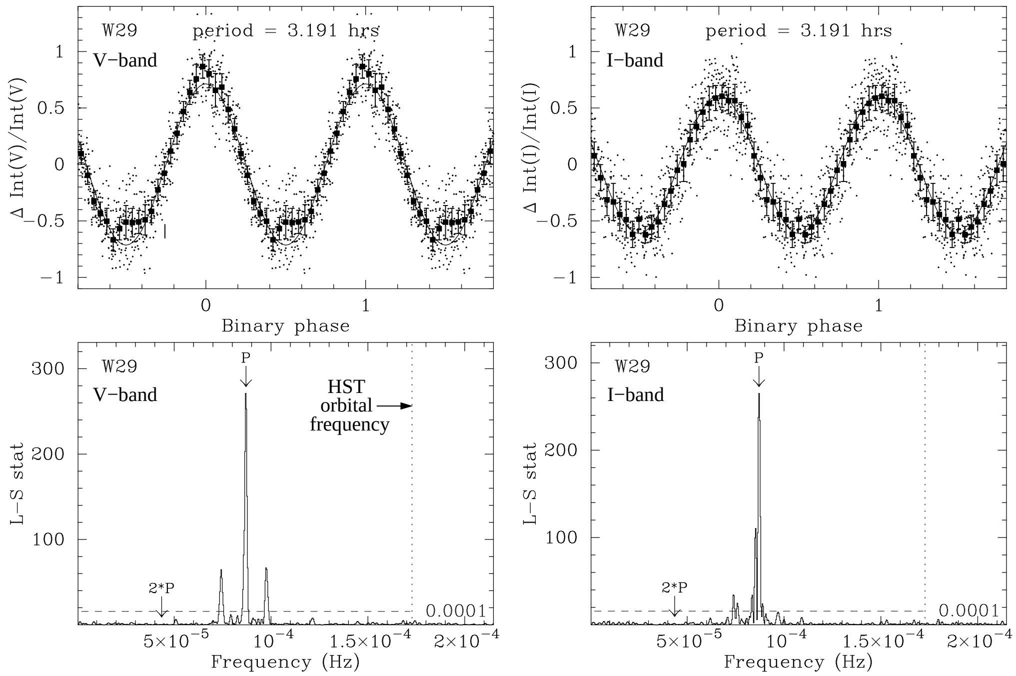

FIG. 4.— Phase plots and power spectra for $W29_{opt}$, using the GO-8267 data. The left side shows the V-band data and the right side the I-band data. The period used to generate the phase plots is slightly (0.02%) higher than the value derived from the GO-8267 data alone, because of improvements based on archival analysis (described in § 2.5.2). The squares show the mean fractional intensity in 25 phase bins between ϕ_b = 0.0 and ϕ_b = 1.0, where the error bars give the 3 σ errors (σ is the standard error in the mean). The solid line shows a sinusoid with the fitted amplitude, period and phase. Note the differences between the V-band data and the sinusoidal model near ϕ_b = 0.0 and ϕ_b = 0.5 (see § 2.5.3). The vertical dotted line in the power spectrum shows the *HST* orbital period (96.4 min) and the horizontal dashed line shows the Lomb-Scargle power corresponding to a false-alarm probability (Scargle 1982) of 1×10^{-4}. The power spectrum peaks near the main period are aliases caused by the *HST* window function.

Note the similarity of the time series (for both filters) to a sinusoid. The power spectrum shows a large peak at the frequency value corresponding to the fitted period, with no evidence for a peak at twice the fitted period. The modulation is thus consistent with arising from a single heated face of the secondary in a circular orbit.

2.5.2. *Use of archival data*

With the above solution as a starting point, we used images from the archive (GO-7503, GO-8219 and SM3/ACS-9028) to refine the orbital solution for the period and phase of $W29_{opt}$. The errors for the period and phase of $W29_{opt}$ from GO-8267 are small enough that the archival data can be included in the orbital solution without any cycle count ambiguity. For example, the 401 day separation between GO-8267 and GO-8219 gives a phase uncertainty of 0.048 d (0.36 of one orbit), when using the error quoted above for the period. Therefore, there is potential to significantly improve our orbital solution using these extra data.

The small set of F555W data from GO-7503 was taken in one contiguous period and spans about 0.85 in phase for $W29_{opt}$. The combination of multi-pixel dithers for the small number of exposures from GO-7503, coupled with the strong variability of $W29_{opt}$, implied that the GO-7503 data itself was not sufficient to generate difference images relative to an internally generated over-sampled mean image. To obtain difference images necessary for extracting variations of $W29_{opt}$ from the GO-7503 data we used the mean, over-sampled image from GO-8267. Positions were fitted to about 50 stars within 7$''$ of $W29_{opt}$ in both the over-sampled reference image and each individual exposure from GO-7503. Transformation coefficients were derived including x,y offsets, rotation and independent plate scales in x,y from the two sets of star positions. Then cubic-spline interpolation in the (essentially noiseless) over-sampled reference image from GO-8267 was used to evaluate an image at the position corresponding to each GO-7503 exposure. Difference images were then formed and the photometry at $W29_{opt}$ was obtained as a 5 pixel sum in each difference image at the calculated position of $W29_{opt}$. Since this is a very crowded region, and the two data sets had an orientation difference of 113°, there was a net (arbitrary) zero point offset removed to force consistency between the relative photometry of the GO-7503 and GO-8267 datasets. The same scale factor (mean intensity of $W29_{opt}$ in the direct image) was used for GO-7503 (compensating for relative exposure times) as for GO-8267, taken with the same filter and detector.

As with the GO-7503 data, there were not enough independent dithers and exposures for GO-8219 to generate good difference images from these data alone. The GO-8219 data were rotated by $\sim$54° relative to GO-8267, and were taken with a different instrument/filter combination. Again, fits were performed for about 50 stars within 7$''$ of $W29_{opt}$ in both the PC1 over-sampled reference image and the individual STIS exposures. Since the STIS CLEAR filter has high response spanning the WFPC2 F555W and F814W filters, we evaluated reference images using cubic spline interpolation from each of these two over-sampled images. The match to STIS data was then evaluated as a linear combination of F555W and F814W reference images and zero point offset, providing a best fit to 50 fiducial stars and several nominal regions representing sky. A mean contribution of 0.437 times V and 0.590 times the I images from PC1 were adopted to best represent the STIS CLEAR data and difference images were formed. To further match the STIS and WFPC2 data images we evaluated and applied convolution kernels attempting to match the relative PSFs. A best solution was found using a convolution kernel that broadened individual STIS PSFs by 10–15% relative to those for the PC1 references. The new difference images were then used in a standard way to extract relative intensity values for $W29_{opt}$ using 5 pixel sums at the calculated position of $W29_{opt}$ in each frame. Here, relative to the WFPC2 data sets, there is an additional uncertainty in normalization of the relative photometry for $W29_{opt}$ at the $\sim$25% level.

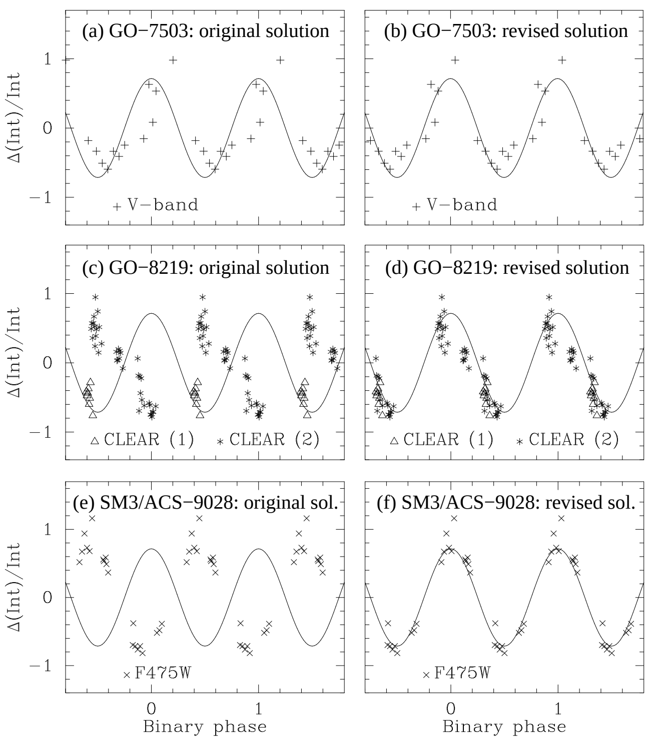

FIG. 5.— Phase plots for archival data from GO-7503, GO-8219 and SM3/ACS-9028. Figure 5a shows the sinusoid derived from the GO-8267 data only (the 'original solution') applied to GO-7503, and Figure 5b shows the revised solution based on the use of all four datasets. Similarly, Figures 5c and 5d show the original and revised solution for GO-8219 (where 'CLEAR (1)' refers to the 1999 data and 'CLEAR(2)' refers to the 2000 data) and Figures 5e and 5f the results for SM3/ACS-9028. Note the dramatic improvement in the results for GO-8219 and SM3/ACS-9028 based on the revised solution.

For SM3/ACS-9028 the improved spatial resolution and PSF for HRC/ACS compared to WFPC2 permitted direct aperture photometry for $W29_{opt}$, rather than difference image analysis (the star is clearly visible in the direct images). The data were dithered by close to half the detector size as part of this calibration program, but $W29_{opt}$ was found in all of the frames.

We then applied the 'original' sinusoidal solution from the 8.3 d of GO-8267 data to the archival time series. Plots of the GO-7503 data ($\sim$110 d after GO-8267) using the above period of 0.132919(16) d (Fig. 5a) showed a slight phase offset requiring a period increase of 0.000025 d ($\sim 1.6\sigma$ using original errors). Plots of the GO-8219 data using the original period (Fig. 5c) showed that after $\sim$401 d the phase error had grown to nearly 0.6, and by the SM3/ACS-9028 data 1002 days later, the phase error had grown to 1.4. Fortunately, the combination of the GO-8267, GO-7503, GO-8219 and SM3/ACS-9028 data allows all four data sets to be phased with no cycle count ambiguity. The resulting period and phase when fitting all four sets of data are P_b = 0.132944(1) d and T_{max} = 51366.8705(3) MJD (see Table 2). By using the archival data the error in the period has been reduced by a factor of 16, with no error change in T_{max}.

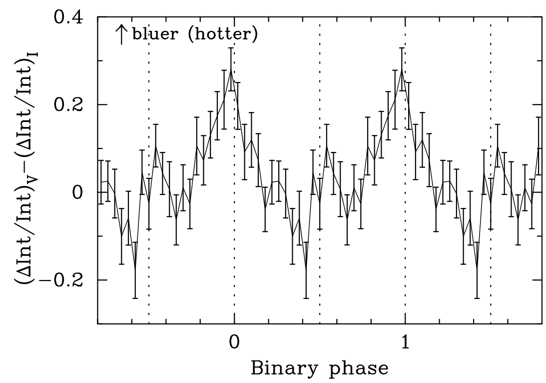

FIG. 6.— The difference between the V and I time series from GO-8267 plotted as a function of phase for $W29_{opt}$. The variable is hottest when it is brightest (ϕ_b = 0.0) and coldest at $\phi_b \sim$0.4.

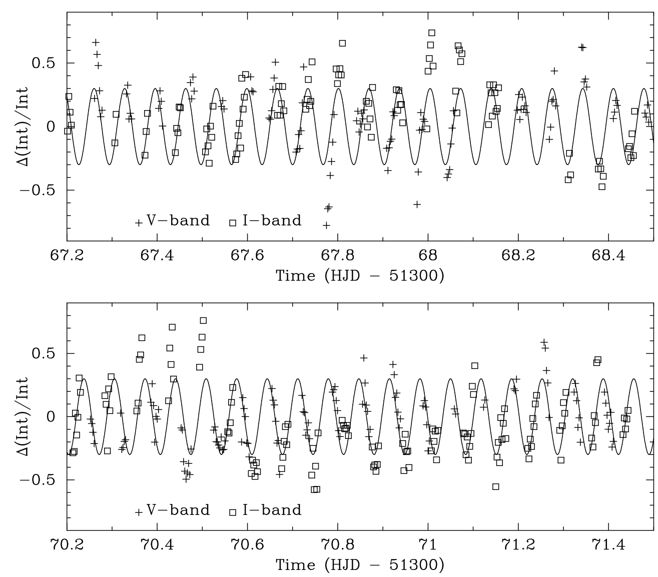

FIG. 7.— Segment of $W34_{opt}$ time series for the GO-8267 data, showing both the V and I time series. A sinusoidal fit to the time series is shown. Note the large deviations from this fit near HJD $\sim$51367.8 and HJD = 51370.35–51370.5.

Using these improved results, the periods of 47 Tuc W and $W29_{opt}$ now differ by 0.000006 d (0.5 s), a difference of 0.2 σ when using the larger (radio) error. Projecting T_{max} for $W29_{opt}$ backwards in time by 1147 orbits, we derive T_{max} = 51214.3837(12) MJD, which differs from the radio-inferred value by only (0.0008 $\pm$ 0.0012) d, a 1.2 minute difference (0.006 in phase). This combination of excellent binary period and phase agreement between $W29_{opt}$ and 47 Tuc W ensures that $W29_{opt}$ is the optical counterpart to the MSP.

2.5.3. *Color changes*

We plot in Figure 6 the difference between the V and I-band relative intensity plots (see Fig. 4) as a function of orbital phase. This figure is equivalent to a $V-I$ color vs phase plot except that increasing y-values correspond to bluer colors (unlike with magnitudes). Note that (*i*) $W29_{opt}$ clearly has a bluer color at $\phi_b \sim$0.0 than at other phases (as expected if the secondary is heated by irradiation from a luminous disk or MSP; see § 3),

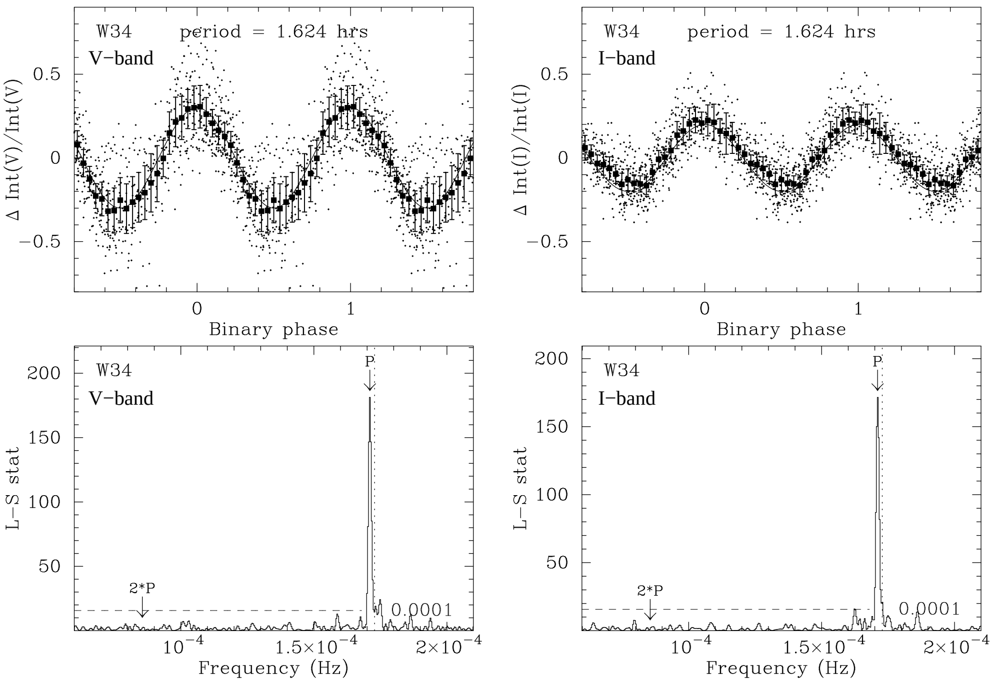

FIG. 8.— Phase plots and power spectra for W34$_{opt}$. As explained in the text the observed period is close to, but statistically different from, the *HST* orbital period.

and (*ii*) the minimum is at ϕ_b ∼0.4, rather than at ϕ_b = 0.5. The main contribution to this possible light curve asymmetry (or excess of V-band signal at ϕ_b ∼0.5) is visible in the V-band plot of Figure 4, where several consecutive points lie above the sinusoidal model near ϕ_b = 0.5. However, given the faintness of W29$_{opt}$ at these phases, it is difficult to confidently declare that this is a real effect.

2.6. *Short Period Variable* W34$_{opt}$

From a review of the optical variables we note that one other star has properties similar to W29$_{opt}$. A faint (V=22.3) star with blue colors ($U-V \sim 0$) shows relatively large amplitude sinusoidal variations in both V and I and is only 4.″9 away from the cluster center. The fit to the GO-8267 time series of this star gives amplitude = 0.301(7), P_b = 0.0676705(78) d, and T_{max} = 51366.5573(3) MJD. The likely *Chandra* counterpart, W34 (Grindlay et al. 2001a), lies 0.″19 (2 σ) away from the optical variable. It has a similar X-ray luminosity to that of W29 (see Table 2), and is also a moderately hard X-ray source, though marginally softer than W29.

Two portions of the time series for W34$_{opt}$ are shown in Figure 7. The large deviations from the sinusoidal model will be discussed in § 3. The phase plots and power spectra for W34$_{opt}$ are shown in Figure 8 and the color vs phase plot in Figure 9. Note from the sinusoidal fit (and Fig. 7) that the period of W34$_{opt}$ (97.45 min) is close to the *HST* orbital period (96.4 min). However, we are convinced that the variations of W34$_{opt}$ are real because: (*i*) the W34$_{opt}$ and *HST* orbital periods differ at almost the 100 σ level, (*ii*) in cases where artifacts of the *HST* orbit are present, there is usually significant power at the harmonics of the *HST* period and at $\pm$(1/86400) Hz, but for W34$_{opt}$ the time series are very clean at the one frequency, (*iii*) since the beat period between 97.45 min and 96.4 min (6.2 d) is shorter than the total observing window (8.3 d), there is a full phase rotation of one cycle in the W34$_{opt}$ signal with respect to the orbit of *HST*, and (*iv*) the mean difference image (difference image at ϕ_b ∼0.0 minus the difference image at ϕ_b ∼0.5) has a stellar shaped PSF, which is only expected if the variation is real, rather than an artifact from a bad pixel interacting with the *HST* orbit-induced motions to generate a false signal.

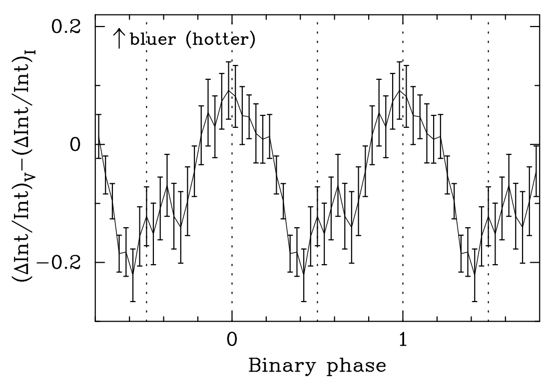

FIG. 9.— The difference between the V and I time series (from GO-8267) plotted as a function of phase for W34$_{opt}$.

3. DISCUSSION

3.1. W29$_{opt}$

As shown above, there is excellent period and phase agreement between W29$_{opt}$ and 47 Tuc W and we regard the association between these two objects as secure. This marks the first time a radio pulsar has been localized with sub-arcsecond precision by means other than radio pulse timing or synthesis observations. We now discuss the nature of W29$_{opt}$ and its variability in the context of all that is known about the binary system, including radio (§ 2.1) and X-ray data.

As noted in § 2.1, the MSP 47 Tuc W was eclipsed for ∼30% of its orbit on the only day in which it was detected at radio wavelengths. The two eclipsing MSPs known in the field (PSRs B1957+20 and J2051–0827, with companion masses of 0.02–

0.03 $M_\odot$) show, to first order, persistent eclipses at similar orbital phases (other eclipsing MSPs with similar binary parameters, in 47 Tuc, are far more poorly studied and relatively little is known in detail about their eclipsing properties). By contrast, the MSPs in NGC 6397 (NGC 6397 A; D'Amico et al. 2001) and Terzan 5 (PSR B1744–24A; Nice & Thorsett 1992) show eclipses that are variable in time and orbital phase. These two systems, while significantly different from each other, are in addition distinct from the other eclipsing MSPs in having larger companion masses, $\sim$0.45 $M_\odot$ and $\sim$0.10 $M_\odot$, respectively.

Naturally we do not know if the eclipses in 47 Tuc W are persistent, but the minimum companion mass of 0.13 $M_\odot$ suggests it is a fundamentally different star from the $\sim$0.02 $M_\odot$ objects. The companion mass is possibly similar to that of 47 Tuc U's companion and other presumed He WD companions to MSPs, but the observed eclipse could not be caused by a He WD companion, and in any case as seen in Figure 2 the photometry for $W29_{opt}$ appears inconsistent with a He WD. The companion mass *is* above the hydrogen burning limit. It therefore appears plausible that $W29_{opt}$ is an MS star, the first such known example as a companion to an MSP (if the companion in NGC 6397 A is an evolved subgiant rather than an MS star).

The large amplitude, nearly sinusoidal light curve of $W29_{opt}$ is reminiscent of the optical light curves of PSRs B1957+20 (Callanan et al. 1995) and J2051–0827 (Stappers et al. 2001). This similarity suggests that the optical variations of $W29_{opt}$ are caused by rotational modulation, as we see alternately the heated and (relatively?) unheated sides of the tidally locked companion once per orbit (as expected, $W29_{opt}$ appears to be hottest when it is brightest; Fig. 6). A similar, large amplitude light curve may also be present in the companion to PSR B1744–24A in Terzan 5, but the formidable reddening and crowding in this cluster (Cohn et al. 2002) have thwarted a recent attempt to detect the companion with *HST* (Edmonds et al. 2001b).

Since the blue color of $W29_{opt}$ probably results from the effects of heating, we have estimated the effects and intensity of the 'radiation bath' $W29_{opt}$ experiences, based on the size of the binary and the expected spin-down luminosity ($\dot{E}$) of 47 Tuc W. Unfortunately, without a timing solution, no direct estimate of $\dot{E}$ is possible. Using the observed X-ray luminosity of 7.8×10^{30} erg s^{-1} and the L_x vs $\dot{E}$ relationship of Grindlay et al. (2002), we estimate that $\dot{E}$ for 47 Tuc W is $\sim 3\times10^{35}$ erg s^{-1} (the 1 σ range is $\sim 2-8\times10^{35}$ erg s^{-1}). A much smaller value of $\dot{E}$ (7.8×10^{33} erg s^{-1}) is derived using the linear relation of Becker & Trümper (1999), $L_x \sim 10^{-3}\dot{E}$, derived largely for field MSPs.

The stellar evolution models of Bergbusch & Vandenberg (1992) give an approximate guide to the relationship between luminosity and mass for a MS star. We adopt the lowest mass model given by Bergbusch & Vandenberg (1992), a 0.15 $M_\odot$ model with T_{eff} = 3300 K and M_V = 13.2, and test whether significant heating of such a star is expected. We use the measured orbital period, an assumed mass for the NS of 1.4 $M_\odot$, and the above secondary mass to estimate the binary separation from Kepler's Third Law. Then, using the estimated secondary radius from the stellar models, and assuming that the MSP radiates its wind isotropically, the 'high' $\dot{E}$ estimate given above implies that the MSP energy intercepted by $W29_{opt}$ should be $\sim 1\times10^{33}$erg s^{-1}, a factor of $\sim 120\times$ the luminosity of the assumed companion (by comparison, the corresponding numbers for the companion to 47 Tuc U are $\sim 7\times10^{30}$erg s^{-1} or $0.013\times$ the luminosity of the companion; EGH01). Assuming that all of the spin-down energy is reradiated as a blackbody, we derive a temperature of 15,500 K. This would imply that heating effects are important and the MS star should be brighter and hotter than in its unperturbed state, possibly explaining the blue colors and relative brightness of $W29_{opt}$.

The above temperature is an upper limit (unless there is beamed emission), since a significant fraction of $\dot{E}$ could be powering other processes such as mass loss. For example, for PSR 1957+20, Callanan et al. (1995) find that the fraction of the MSP flux intercepted by the secondary that is converted into optical emission (defined as η) is either in the range 0.07–0.2 for a Roche lobe filling model, or $\eta \gtrsim 3$ (significant beaming) for a secondary considerably underfilling its Roche lobe. Stappers et al. (2001) find $\eta \sim$0.3 for J2051–0827 and EGH01 find $\eta \sim 1$ for 47 Tuc U. Guided by these numbers we assume a conservatively small value for η of $\sim$0.1 to give a reasonable lower limit on the heating flux, and derive a blackbody temperature of $\sim$8,700 K. Therefore heating effects should still be important.

For this model, the ratio between the heating flux and the undisturbed luminosity of the assumed stellar companion (120) is only a factor of 2.4 larger than the ratio (caused by heating) between the V-band flux of $W29_{opt}$ and the V-band flux of the stellar model (implying $\eta \sim$0.4). However, if this model is approximately correct, the relatively small difference in intensity between the heated and unheated sides of $W29_{opt}$ (a factor of 6 compared to the above factor of 120) has to be explained. One possibility is that heating of the companion has occurred fairly evenly over its surface. Although the secondary is probably tidally locked, significant heating of the darker side of the star might be expected because of energy transport within the star from the combined effects of convection (this low mass MS star should be fully convective), and the effects of relativistic e^+e^- pairs and γ-ray photons (D'Antona 1996). It is also possible that a crescent of the heated hemisphere is visible at all orbital phases if the orbital inclination of the binary is significantly less than 60° (Fruchter et al. 1995). This requires a higher mass companion for consistency with the radio results and the brighter star also gives a correspondingly smaller amplitude. In the case of NGC 6397 A, where the inclination is known to be high, the companion also has a much smaller variability amplitude than expected based on heating estimates (Orosz & van Kerkwijk 2002). This may be a feature common to all MSP systems containing non-degenerate companions.

Approximate upper limits to the mass and radius of the 47 Tuc W companion are set by the requirement that mass transfer be avoided. Using the Roche-lobe formula from Paczyński (1971) ($r/a = 0.462[(M_W/(M_{NS}+M_W)]^{1/3}$, where r is the Roche-lobe radius, a is the binary separation, M_W is the mass of the secondary and M_{NS} is the mass of the NS), we derive that, in its unperturbed state, a 0.29 $M_\odot$ model with T_{eff}= 3680 K and M_V = 10.8 would underfill its Roche lobe by $\sim$1% (the corresponding upper limit on the orbital inclination is 27°). Our 0.15 $M_\odot$ model would (in its unperturbed state) significantly underfill its Roche lobe (the ratio of the stellar radius to r is 0.6), explaining why the NS is not accreting. However, under the influence of the extreme radiation bath from the MSP, $W29_{opt}$ may expand to fill or almost fill its Roche lobe (D'Antona & Ergma 1993), with accretion being inhibited by radiation pressure from the MSP (as may be occuring in NGC 6397 A; Burderi et al. 2002).

Using the 'low' $\dot{E}$ estimate given above, the MSP energy intercepted by $W29_{opt}$ is only $\sim 4\times10^{31}$erg s^{-1} (with a reradiated blackbody temperature of 6,300 K), a factor of $\sim$3.3 times the luminosity of the assumed companion. This luminosity ratio is smaller than the observed variation and is a factor of 15 *smaller* than the ratio between the V-band flux of W29$_{\rm opt}$ and the V-band flux of the stellar model. So, unless significant beaming is present, only a fainter MS star than assumed above can give a larger ratio between the heating flux and the stellar luminosity. However, the disparity between the V-band fluxes then increases by the same amount. A smaller ratio between the V-band fluxes is given by a brighter, more massive secondary (requiring an inclination $< 60°$), but then the heating flux would be too small to cause the observed variations. These inconsistencies suggest that the higher $\dot{E}$ value given earlier is closer to the true value, providing indirect support for the L_x vs $\dot{E}$ relationship of Grindlay et al. (2002).

The similarities between the X-ray properties of W29 and those of the X-ray counterparts of NGC 6397 A (see § 2.3) and 47 Tuc J offer valuable insight. These similarities at the very least allow for a similar physical origin of the X-ray emission. The extended nature of the hard X-ray source in NGC 6397 A suggests it is due to shocked gas lifted from the binary companion (Grindlay et al. 2002), and similar behavior may be occurring in W29. This match in X-ray properties between W29 and two other eclipsing MSPs suggests evidence for a trend, since apart from 47 Tuc J, all 9 of the X-ray-detected MSPs in 47 Tuc that are bright enough to have useful hardness ratios determined have soft spectra (caused by likely thermal emission from their polar caps; Grindlay et al. 2002).

As we have already mentioned, 47 Tuc W is an extremely unusual (and so far possibly unique) MSP in having a likely MS companion. This likely represents evidence for stellar interactions, not surprising for a system so close to the cluster center. One possible formation scenario for this system is that an NS was spun up by accretion to form an MSP, which eventually evolved into an MSP/very low mass companion binary. Later, a collision between the MSP binary and the currently observed MS star caused the very low mass star (the lightest object amongst the 3 stars) to be ejected from the system. Alternatively, a single MSP could have exchanged into a double MS star binary, although in this case tight constraints on the mass of the ejected star may be necessary unless W29$_{\rm opt}$ was once considerably more massive than it is today. Significant mass loss could be taking place if W29$_{\rm opt}$ is close to filling its Roche lobe and material is being expelled from the system under the propeller mechanism (Burderi et al. 2002). A third possibility is that the observed binary was formed as a result of direct 2-body tidal capture (Mardling 1995) between a single MSP and an MS star, although this process may be much less important than binary interactions (Rasio et al. 2000).

In testing these various exchange scenarios, we note that 47 Tuc W is located very close to the cluster center (only $3\farcs8$ or $0.16r_c$ away), consistent with the centrally concentrated spatial distribution of the other MSPs. If the MSP was initially ejected from the cluster core in an exchange encounter it may have had time to sink back into the cluster core, since the MS star could have been captured several Gyr ago, and the central relaxation time for 47 Tuc is 0.1 Gyr (increasing to 3 Gyr at the half-mass radius of $2\farcm8$; Harris 1996). The NGC 6397 MSP, by contrast, is found $\sim$30$''$ from the cluster center (Ferraro et al. 2001) and is therefore well outside the cluster core ($r_c = 3\farcs0$; Harris 1996), possibly showing evidence for ejection from the core (D'Amico et al. 2001; Grindlay et al. 2002). This ejection may have occurred quite recently, since the central relaxation time for the core-collapsed NGC 6397 is only 0.08 Myr, increasing to 0.3 Gyr at the half-mass radius of $2\farcm3$ (Harris 1996). If these numbers are accurate, a system as heavy as NGC 6397 A should sink rapidly back into the core (unless it is in a highly elliptical orbit). One possible explanation is that NGC 6397 A was formed very recently by an NS capturing a subgiant, and was ejected from the core in this interaction. This scenario is broadly consistent with the relatively small (characteristic) age for the system of 0.35 Gyr (D'Amico et al. 2001). It may also have been ejected from the cluster core in a subsequent interaction. A similar ejection scenario may apply to PSR B1744–24A, which is located $\sim 40''$ from the center of Terzan 5 (Nice & Thorsett 1992), equivalent to $\sim 5r_c$ using the recent r_c determination by Cohn et al. (2002).

It may be possible that W29$_{\rm opt}$ will eventually fill its Roche lobe and cause mass accretion onto the NS to recommence, as may occur for NGC 6397 A (Ferraro et al. 2001 and Burderi et al. 2002). In this scenario, as W29$_{\rm opt}$ keeps losing mass, it eventually may end up like the very low mass (0.02–0.03 $M_\odot$) systems such as 47 Tuc J (though these may be ablated He WDs rather than ablated MS stars; Rasio et al. 2000). Then, after continued ablation, it could possibly become an isolated MSP.

3.2. W34$_{\rm opt}$

Unlike with W29$_{\rm opt}$, there is no period or phase match for W34$_{\rm opt}$ with a known MSP (its period is similar to, but statistically different from, the 95.39 $\pm$ 0.1 min period of 47 Tuc R, an eclipsing MSP with a very low mass companion; CLF00), but a significant fraction of the 47 Tuc MSPs have not yet been detected in the radio (CLF00; Grindlay et al. 2002). Given the short period of this system, the heating effects (if it is an MSP) may be even more dramatic than for W29$_{\rm opt}$, since the ratio between the heating flux and the stellar luminosity would be higher, assuming a similar luminosity companion star. We note that the color difference between the brighter and darker sides of the companion ($\sim$30%) compared to the amplitude of the variation is larger than the similar ratio for W29$_{\rm opt}$. The smaller amplitude of W34$_{\rm opt}$ compared to W29$_{\rm opt}$ may simply be an inclination effect or it may reflect a significant difference in the level of heating of the dark side of the companion, or show evidence for a different type of star, such as a very low mass degenerate star instead of an MS star. We also note that in this system the low mass model assumed above for W29$_{\rm opt}$ would overfill its Roche lobe by a few percent.

There are broad similarities in the appearance of the color vs phase plots for W29$_{\rm opt}$ (Fig. 6) and W34$_{\rm opt}$ (Fig. 9), particularly in the positions of the peak near ϕ_b = 0.0, the minimum at $\phi_b \sim$0.4, and the possible 'hump' of relatively blue light at ϕ_b = 0.4–0.7. The relatively blue color at optical maximum is secure, but the effects near ϕ_b = 0.5 can only be considered marginal, given the faintness of the stars at these times and the possibility that artifacts of the *HST* orbit may have leaked into the time series (half the period of W29$_{\rm opt}$ is 95.72 min).

These comparisons do not constitute proof that W34$_{\rm opt}$ is an MSP companion, and therefore we briefly consider alternative explanations for its behavior. The near-sinusoidal light curve of W34$_{\rm opt}$, with its short period and large amplitude, is similar to that of a W UMa variable (a contact, or near contact binary consisting of two MS stars). However, this interpretation is clearly inconsistent with the blue colors of this object. A second possible explanation is that W34$_{\rm opt}$ is a CV, since most of the CVs in 47 Tuc (and also most of the CVs in NGC 6397 and the field) are optically variable blue stars with moderately hard X-ray counterparts (Grindlay et al. 2001a). However, the likely CVs in 47 Tuc show flickering (random fluctuations on timescales of minutes with amplitudes of $\sim$0.05–0.1 mag) which hides the presence of periodic variations in most cases. Of the few CVs in 47 Tuc which do show periodic variations, the light curves are very different from those of $W34_{opt}$ (and $W29_{opt}$), and show either low amplitude ($\lesssim$ 0.1 mag) periodic variations from ellipsoidal modulation, or a combination of ellipsoidal modulation and eclipses (Edmonds et al. 2002a, in preparation), with distinctly non-sinusoidal light curves (there is significant signal in the power at both the orbital period and half the orbital period). Given these differences, then unless $W34_{opt}$ is a different type of CV from the $\sim$20 good candidates found in 47 Tuc, we consider it more likely to be an MSP.

As shown in Figure 7, there are several instances of large deviations from the sinusoidal model for $W34_{opt}$. We examined the standard deviation of the residuals (data–sinusoid) for each cycle of the $W34_{opt}$ light curve, after iteratively removing 3 σ deviations from the mean, and compared these results with those found for $W29_{opt}$. The mean standard deviation for $W34_{opt}$ (0.15) was similar to the value found for $W29_{opt}$ (0.21), but there were some differences in the distributions. No 3 σ deviations were found for $W29_{opt}$, but two were found for $W34_{opt}$ (at HJD $\sim$51363.6 and HJD $\sim$51367.8), and two consecutive cycles of $\sim 2.9\sigma$ deviations (in HJD = 51370.35–51370.5) were also found. These variations could be evidence for variable mass loss from the companion or they could be episodes of unusually large flickering, if the CV model is correct.

4. SUMMARY AND FUTURE OBSERVATIONS

Briefly summarizing the key results in this paper, we have identified a binary companion, $W29_{opt}$, to a second MSP in the cluster 47 Tuc (adding to the detection of a He WD companion to MSP 47 Tuc U; EGH01). This faint, blue star shows large amplitude sinusoidal variations in both *V* and *I* (caused by heating of a tidally locked companion), and has a period and phase which match remarkably well with those of the MSP 47 Tuc W. We argue, based on the radio and optical results, that $W29_{opt}$ is a main sequence star, a rare circumstance for an MSP companion, and we present evidence for another optical variable (with similar properties to $W29_{opt}$) that may also be an MSP companion.

Deeper *Chandra* observations of 47 Tuc scheduled for 2002 September (PI J. Grindlay) will allow variability and spectral studies of W29, with dependences on phase, to be made. Simultaneous observations scheduled with ACS (as part of the same program) will provide the first *HST* images of 47 Tuc in H_α, and should detect evidence for a strong emission line in $W34_{opt}$ if it is a CV rather than an MSP companion. Combination of this data with archival data and with the GO-8267 time series will refine the period and phase of $W34_{opt}$. Finally, by combining these X-ray data with existing and future *HST* observations of 47 Tuc, more MSP companions may be identified.

We thank Andy Fruchter and Kailash Sahu for discussions, and the referee Scott Ransom for helpful comments. This work was supported in part by STScI grant GO-8267.01-97A (PDE and RLG) and NASA grants NAG 5-9095 and SAO grant GO1-2063X (FC).

REFERENCES

Albrow, M. D., Gilliland, R. L., Brown, T. M., Edmonds, P. D., Guhathakurta, P., & Sarajedini, A. 2001, ApJ, 559, 1060
Becker, W. & Trümper, J. 1999, A&A, 341, 803
Bergbusch, P. A. & Vandenberg, D. A. 1992, ApJS, 81, 163
Bergeron, P., Wesemael, F., & Beauchamp, A. 1995, PASP, 107, 1047
Burderi, L., D'Antona, F., & Burgay, M. 2002, ApJ, in press (astro-ph/0203387)
Callanan, P. J., van Paradijs, J., & Rengelink, R. 1995, ApJ, 439, 928
Camilo, F., Lorimer, D. R., Freire, P., Lyne, A. G., & Manchester, R. N. 2000, ApJ, 535, 975 (CLF00)
Cohn, H. N., Lugger, P. M., Grindlay, J. E., & Edmonds, P. D. 2002, ApJ, 571, 818
D'Amico, N., Possenti, A., Manchester, R. N., Sarkissian, J., Lyne, A. G., & Camilo, F. 2001, ApJ, 561, L89
D'Amico, N., Possenti, A., Fici, L., Manchester, R. N., Lyne, A. G., Camilo, F., & Sarkissian, J. 2002, ApJ, 570, L89
D'Antona, F. 1996, NATO ASI Proc. 477: Evolutionary Processes in Binary Stars, 287
D'Antona, F. & Ergma, E. 1993, A&A, 269, 219
Edmonds, P. D., Gilliland, R. L., Heinke, C. O., Grindlay, J. E., & Camilo, F. 2001a, ApJ, 557, L57 (EGH01)
Edmonds, P. D., Grindlay, J. E., Cohn, H., & Lugger, P. 2001b, ApJ, 547, 829
Edmonds, P. D., Heinke, C. O., Grindlay, J. E., & Gilliland, R. L. 2002b, ApJ, 564, L17
Ferraro, F. R., Possenti, A., D'Amico, N., & Sabbi, E. 2001, ApJ, 561, L93
Freire, P. C. 2001, Ph.D. thesis, Univ. Manchester
Freire, P. C., Camilo, F., Lorimer, D. R., Lyne, A. G., Manchester, R. N., & D'Amico, N. 2001a, MNRAS, 326, 901
Freire, P. C., Kramer, M., Lyne, A. G., Camilo, F., Manchester, R. N., & D'Amico, N. 2001b, ApJ, 557, L105
Fruchter, A. S., Bookbinder, J., & Bailyn, C. D. 1995, ApJ, 443, L21
Gilliland, R. L., et al. 2000, ApJ, 545, L47
Grindlay, J. E., Heinke, C. O., Edmonds, P. D., & Murray, S. 2001a, Science, 292, 2290
Grindlay, J. E., Heinke, C. O., Edmonds, P. D., Murray, S. S., & Cool, A. M. 2001b, ApJ, 563, L53
Grindlay, J. E., Camilo, F., Heinke, C. O., Edmonds, P. D., Cohn, H., & Lugger, P. 2002, ApJ, submitted
Harris, W. E. 1996, AJ, 112, 1487
Holtzman, J. A., Burrows, C. J., Casertano, S., Hester, J. J., Trauger, J. T., Watson, A. M., & Worthey, G. 1995, PASP, 107, 1065
Lyne, A. G., et al. 1990, Nature, 347, 650
Manchester, R. N., Lyne, A. G., Robinson, C., Bailes, M., & D'Amico, N. 1991, Nature, 352, 219
Mardling, R. A. 1995, ApJ, 450, 722
Nice, D. J. & Thorsett, S. E. 1992, ApJ, 397, 249
Orosz, J. A. & van Kerkwijk, M. H, 2002, A&A, submitted
Paczyński, B. 1971, ARA&A, 9, 183
Rasio, F. A., Pfahl, E. D., & Rappaport, S. 2000, ApJ, 532, L47
Robinson, C. R., Lyne, A. G., Manchester, A. G., Bailes, M., D'Amico, N., & Johnston, S. 1995, MNRAS, 274, 547
Scargle, J. D. 1982, ApJ, 263, 835
Serenelli, A. M., Althaus, L. G., Rohrmann R. D., & Benvenuto, O. G. 2001, MNRAS, 325, 607
Stappers, B. W., van Kerkwijk, M. H., Bell, J. F., & Kulkarni, S. R. 2001, ApJ, 548, L183
Zoccali, M., et al. 2001, ApJ, 553, 733

TABLE 1

SUMMARY OF OPTICAL DATA

Dataset	Observation Date	Camera	Filters	Exposures
GO-8267	1999 July 3–11	WFPC2	F555W (‘*V*’)	636×160 s
		WFPC2	F814W (‘*I*’)	653×160 s
GO-7503	1999 October 28	WFPC2	F555W	9×40 s; 3×120 s[a]
GO-8219	1999 September 10	STIS	CLEAR	8×30 s
	2000 August 7–16	STIS	CLEAR	38×30 s
SM3/ACS-9028	2002 April 5	ACS/HRC	F475W	20×120 s

[a]The 40 s exposures were composed of co-added 20 s exposures

TABLE 2

OPTICAL, RADIO AND X-RAY DATA FOR THE COMPANION TO MSP 47 TUC W ($W29_{opt}$) AND A CANDIDATE MSP COUNTERPART ($W34_{opt}$)

Source	RA[a] (J2000)	Dec[a] (J2000)	U	V	I	P_b (days)	T_{max}[b] (MJD)	L_X[c] (erg s^{-1})	X-ray spectrum[c] (photon index)
$W29_{opt}$	00 24 06.07(1)	−72 04 49.02(6)	23.8(5)	22.3(2)	21.6(3)	0.132944(1)[d]	51366.8705(3) 51214.3837(12)[e]	7.8×10^{30}	1.8 ± 0.6
47 Tuc W	. . .	. . .	. . .	. . .	. . .	0.13295(4)[f]	51214.38454(3)[g]	. . .	. . .
$W34_{opt}$	00 24 05.21(2)	−72 04 46.59(6)	22.3(5)	22.3(3)	21.6(4)	0.0676705(78)	51366.5573(3)	4×10^{30}	$2.4^{+0.5}_{-0.6}$

[a]Coordinates are in the JPL DE200 planetary ephemeris frame used for MSP timing (Freire et al. 2001a)

[b]Time of optical maximum (see text)

[c]L_X and the spectral fit assume cluster $N_H = 3.0\times10^{20}\,\mathrm{cm}^{-2}$

[d]Binary period derived from optical data

[e]Optical T_{max} − 1147 orbits

[f]Binary period derived from radio data

[g]T_{max} derived from radio data